Nonlinear Mesoscopic Elasticity: Evidence for a New Class of Materials

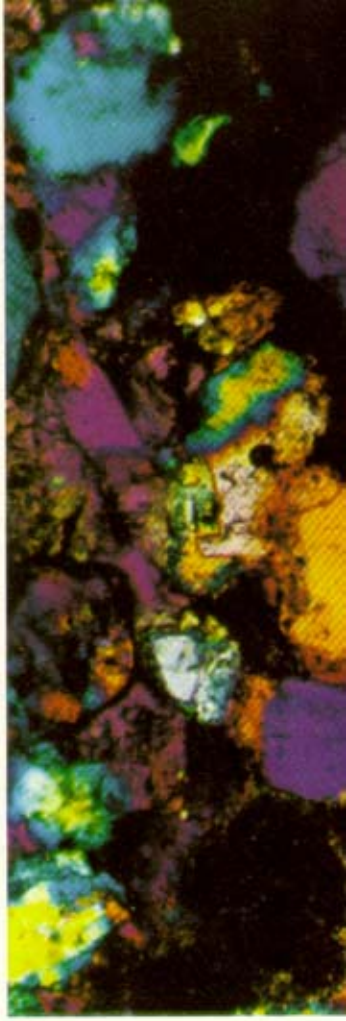

New tools such as nonlinear resonant ultrasound spectroscopy are being used to reveal the complex behavior of rocks and other materials.

Robert A. Guyer and Paul A. Johnson

A squash ball almost doesn't bounce; a Superball bounces first left then right, seeming to have a mind of its own. Remarkable and complex elastic behavior isn't confined to sports equipment and toys. Indeed, it can be found in some surprising places. When the elastic behavior of a rock is probed, for instance, it shows extreme nonlinearity hysteresis and discrete memory (the Flintstones could have had a computer that used a sandstone for random-access memory). Rocks are an example of a class of unusual elastic materials that includes sand, soil, cement, concrete, ceramics and, it turns out, damaged materials. Many members of this class are the blue-collar materials of daily life: They are in the bridges we cross on the way to work, the roofs over our heads and the ground beneath our cities—such as the Los Angeles basin (home to many earthquakes). The elastic behavior of these materials is of more than academic interest.

Rocks are examples of consolidated materials—that is, they are materials whose primary physical properties are a consequence of the process of their assembly. For example, a sandstone is an aggregate of grains (composed of a single mineral or a group of minerals) that are fused together by temperature, pressure and chemical processes. The cover of this issue and figure 1 show the structure of Berea sandstone, which we study below.

In a sandstone the grains themselves act as rigid units, while the contacts between grains—the bond system—constitute a set of effective elastic elements that control the elastic behavior of the sandstone. These elastic elements, heterogeneous in size and shape, are mesoscopic, with a typical size of 1 μm. Materials whose elastic properties are determined by such a bond system are called nonlinear mesoscopic elastic (NME) materials. Igneous and metamorphic rocks are also NME materials. Their bond systems consist of a fabric of defects (cracks) that participates in the elastic response of the rocks.

ROBERT GUYER *is a professor of physics at the University of Massachusetts, Amherst.* PAUL JOHNSON *is a member of the technical staff at the Los Alamos Seismic Research Center at Los Alamos National Laboratory in New Mexico.*

NME materials stand in sharp contrast to materials such as aluminum, diamond and water that have atomic elasticity which arises from atomic-level forces between atoms and molecules. Materials with atomic elasticity are well described by the traditional theory of elasticity. However, the theory does a poor job of describing the elastic properties of NME materials. In this article, we discuss new tools and models being developed to better characterize these materials, and present practical uses for our improved understanding of their behavior.

Quasistatic nonlinearity

The most fundamental elastic properties of a material are seen in the quasistatic equation of state, the stress–strain relationship. In figure 2 we compare the strain ε (the fractional change in length) as a function of the applied stress σ for an NME material, Berea sandstone, and an atomic elastic material, glass. Although there is scant evidence for nonlinearity in glass at stresses up to at least 25 megapascals, the sandstone is highly nonlinear and hysteretic at these moderate stresses. Referring to the figure, when the stress on the sandstone is decreased at point B, the strain only partially reverses—most of the strain stays in. A hysteresis loop with a cusp at B develops. This loop closes when the stress is returned to zero.

As shown in figure 2b, the stress is reversed seven times in the course of the measurements. These reversals produce the small, interior hysteresis loops labeled $1 \cdots 7$ in figure 2a. Details of the third reversal are shown in figure 2c. Note that when the stress reaches σ_3 for the second time, the strain returns to the trajectory it was originally on before it traced the interior loop. This is the phenomenon of "discrete memory" (or endpoint memory) familiar from magnetism, capillary condensation and the elasticity of shape-memory alloys. Along with high nonlinearity and hysteresis, discrete memory is one of the

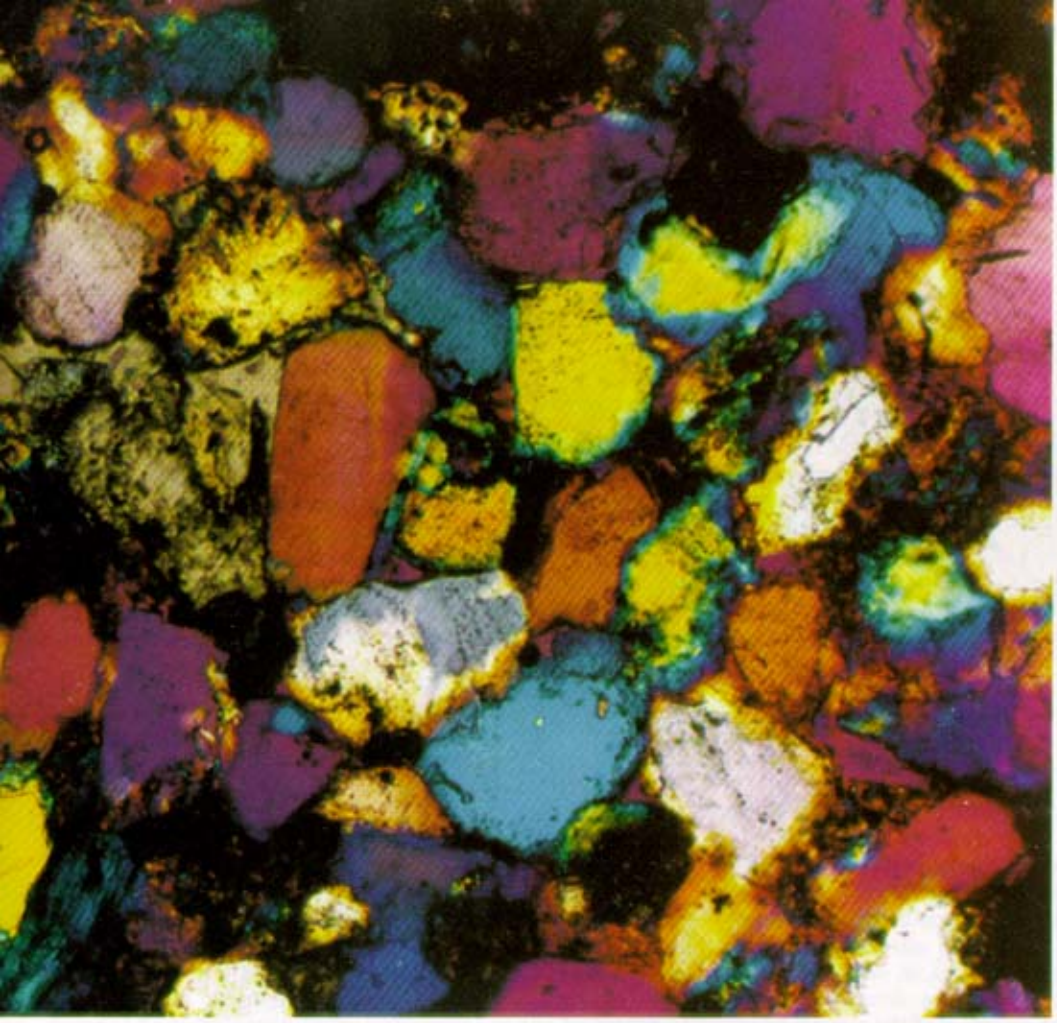

FIGURE 1. GRAIN STRUCTURE and bond system of Berea sandstone. This photomicrograph was obtained from a slice of Berea sandstone only 30 μm thick. Illumination with cross-polarized light produced this colorful display, which provides information about the size, composition and orientation of the grains. Grain diameters range from 0.05 to 0.2 mm. Most of the grains are quartz, although feldspar and mica are also present. The grains are cemented by silica and calcite. The contacts between the grains constitute the rock's bond system.

signatures of nonlinear mesoscopic elasticity

A phenomenological explanation of the stress–strain relationship for rocks has been developed by one of us (Guyer) and Katherine McCall.[1] In box 1 on page 33, the rudiments of this model, called the P–M space model, are outlined and the important features seen in a stress–strain curve like that of sandstone are described.

Dynamic elasticity and the wave equation

We've seen that quasistatic measurements on NME materials such as sandstone show evidence for unusual elastic properties, including extreme nonlinearity hysteresis and discrete memory. What is the dynamic elastic response of a rock? How do sound waves propagate in a rock?

The traditional theoretical formulation of dynamic elasticity both linear and nonlinear (found, for example, in reference 2), has been highly developed in the former Soviet Union and elsewhere.[3] This formulation relates the time evolution of the local displacement (the displacement field) to a Taylor expansion in the strain and takes the form of a nonlinear wave equation (see box 2 on page 34).

A basic physical process brought about by nonlinearity in the wave equation is the coalescence of strain fields within the material. For example, two strain waves with frequencies ω_1 and ω_2 and amplitudes ε_1 and ε_2 can coalesce to form a strain wave with frequency components $\omega_\pm = \omega_1 \pm \omega_2$ and amplitude proportional to $\varepsilon_1\varepsilon_2$. Experiments that look for coalescence, and that probe the scaling of the detected signal with $\varepsilon_1\varepsilon_2$ and distance of propagation, are the hallmark of nonlinear acoustics[3] (and also nonlinear optics).

Propagating-wave experiments of this type conducted in rock have provided qualitative support for predictions from the nonlinear wave equation. Rarely though, have they provided quantitative measures of dynamic nonlinear elasticity[4] One problem is that an applied stress may be conducted nonuniformly through a heterogeneous material, leading to dispersion caused by wave velocities that vary with stress path.[5] (See the article on granular materials in PHYSICS TODAY, April 1996, page 32.) Also, many rocks have high intrinsic attenuation.

Resonant-wave experiments, on the other hand, have proved to be a valuable quantitative probe of the nonlinear elastic state of a rock because of the self-amplification that resonance provides. In these experiments, a rod-shaped sample has an ultrasound transducer fixed at one end and an accelerometer attached to the other. For a given drive level, the acceleration is recorded as the frequency of the applied wave is swept from above to below the fundamental resonance mode of the sample. This type of nontransient dynamic experiment we term nonlinear resonant ultrasound spectroscopy (NRUS) after the work of Orson Anderson, Albert Migliori and others who developed linear resonant ultrasound spectroscopy[6] (See the article on resonant ultrasound spectroscopy in PHYSICS TODAY, January 1996, page 26.)

In figure 3, we compare the resonance response curves of materials with atomic and nonlinear mesoscopic elasticity. The contrast is striking. For Lucite, there is no change in the shape of the resonance curve with increase in drive level (at least to the unaided eye), implying a linear response out to acceleration amplitudes of at least 500 m/s^2. For Berea sandstone, even at an acceleration amplitude of 50 m/s^2, there is noticeable distortion of the resonance curves. In figure 3c, we see evidence of a shift in the resonant frequency down to the smallest strains we can measure (ε of order 10^{-8}). Remarkably there appears to be no threshold to nonlinear behavior.

Besides qualitative evidence for the presence of nonlinearity what can we learn from NRUS experiments? When the traditional theory of nonlinear elasticity is

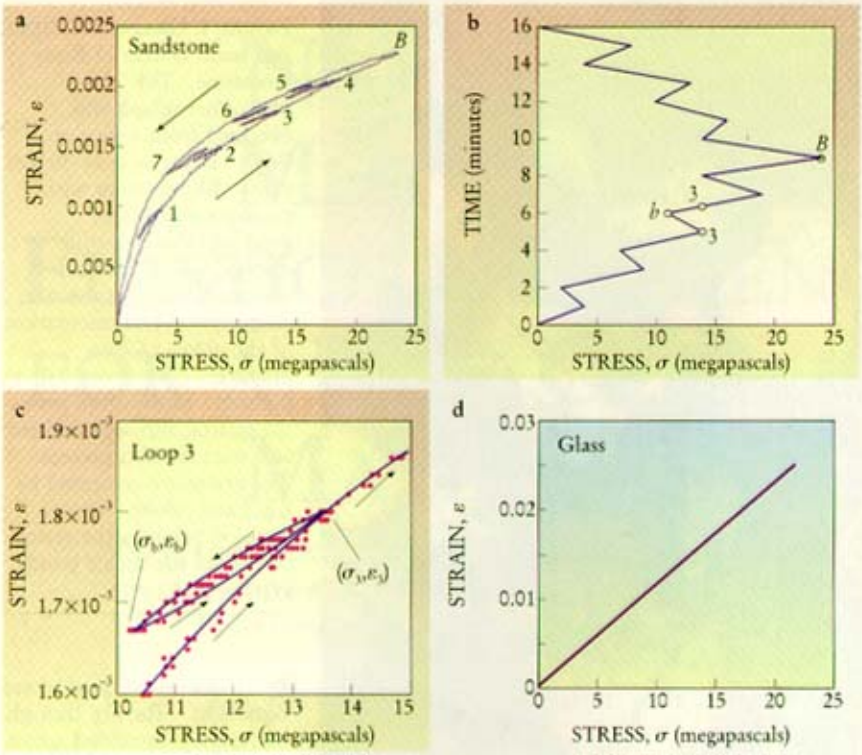

FIGURE 2. STRESS-STRAIN RELATIONSHIPS for nonlinear mesoscopic and atomic elastic materials. **a:** The strain ε as a function of the applied stress σ for Berea sandstone, a material with nonlinear mesoscopic elasticity (data courtesy of Brun Hilbert). **b:** The history of the stress. Seven stress reversals produced the small, internal hysteresis loops of **a**, which were traversed in the same sense as the large loop. **c:** The stress-strain relationship for loop 3 (red dots), generated by the reversal $3 \rightarrow b \rightarrow 3$ in the stress history. The blue line shows the loop trajectory. **d:** In contrast, the stress-strain curve is essentially linear for optical-grade glass (BaK-1, Schott Glass Technologies Inc), an atomic elastic material (data courtesy of Greg Boitnott).

applied to a resonant bar; the nonlinear behavior is found to be due to quartic anharmonicity (the δ term in box 2) in which three strain fields of amplitude ε and frequency ω coalesce to form a strain field with amplitude ε^3 and frequency components $\pm\omega \pm \omega \pm \omega = 3\omega, \omega, -\omega, -3\omega$. The $\pm\omega$ components of this strain field are detected in the resonance experiments. As a consequence of the quartic term, a shift in the resonant frequency proportional to both δ and ε^2 is expected. Instead, however, we see a frequency shift directly proportional to $|\varepsilon|$ (see figure 3c). This unexpected result, we have come to realize, is a principal dynamic signature of nonlinear mesoscopic elasticity.

To understand this signature, we must return to the quasistatic data shown in figure 2. The hysteresis and discrete memory observed there are explained in terms of an assemblage of hysteretic elastic elements (see box 1). When these hysteretic elastic elements are included in the description of the dynamic response of the rock, leading to the term $A[\varepsilon, \dot{\varepsilon}]$ in the wave equation of box 2, the theory of the behavior of a resonant bar yields results in qualitative *and* quantitative accord with experiment.[1] Thus there seems to be a coherent description of the elastic properties of rocks that includes both quasistatic behavior (figure 2) and dynamic behavior (figure 3) that extends over at least five orders of magnitude in strain and six orders of magnitude in frequency. The essential feature in this description is a bond system of hysteretic elastic elements.

As always, the story is more complicated. Very careful NRUS measurements carried out recently reveal the presence of a "slow dynamics" in the elastic response of a rock.[7] As we have seen, when a sample is driven by a large amplitude, the resonant frequency will shift downward in proportion to the drive level. After terminating the large amplitude drive, the low-amplitude resonance frequency is found to shift back to its original value over a period ranging from tens of minutes to hours. Characterization of this behavior is one subject of current research. Slow dynamics may prove to be a second dynamic signature of nonlinear mesoscopic elasticity.

We do not have a complete understanding of the cause of the elastic properties we have been describing. An essential feature seems to be hysteretic elastic elements in the bond system. However, the mechanism of hysteresis is elusive. Significant efforts in the investigation of NME materials are focusing on these issues.

Fortunately we do not need full understanding of the cause and mechanism of nonlinear mesoscopic elasticity to study interesting and practical realizations of it. Let us turn from rocks and look more broadly at other NME materials, at nonlinear mesoscopic elasticity near Earth's surface, and at nondestructive evaluation (NDE) of damage in materials.

Nonlinear mesoscopic elasticity at work

Do the elastic properties we have illustrated with rocks characterize an elasticity universality class consisting not only of rock but also of concrete, sand, soil and other materials? This is an attractive proposition. Many of the materials we could consider placing in this class have not had their elastic properties scrutinized as closely as rocks have. All are known to share with rocks at least one of the three main characteristics: large nonlinearity, hysteresis and discrete memory. As an example, the resonant responses of Lavoux limestone, concrete and cracked synthetic slate all show (figure 4) a frequency shift with amplitude (always softening) similar to that observed in sandstone (figure 3c). The frequency shifts are proportional to the drive level, a signature of nonlinear mesoscopic elasticity. The premise of an elasticity universality class may have some merit.

One promising application of NME models is in the study of ground motion in earthquakes. Such naturally occurring events can be catastrophic. For example, in addition to causing devastating human loss, the Kobe earthquake that hit the southern part of Japan's Hyogo prefecture on 17 January 1995 was estimated to cause damage totaling over $100 billion. Approximately 150 000 buildings collapsed, and the Kobe port—the second largest in Japan—was effectively closed by the earthquake. It was the costliest earthquake in history.

The most damaging aspect of a large earthquake is strong ground motion that couples into resonant modes of structures and causes their failure.[8] In box 3 on page 35, we illustrate the typical circumstance that leads to strong ground motion: a layer of soil—a nonlinear elastic mate-

Box 1. A Phenomenological Model of Nonlinear Mesoscopic Materials

Based on the work of Franz Preisach and Isaac Mayergoyz,[17] one of us (Guyer) and Katherine McCall[1] have developed a phenomenological model to describe the quasistatic stress–strain relationship in rocks. In this model, called the P–M space model, the bond system of a rock is represented as an assemblage of hysteretic elastic elements that can be in only one of two states, open or closed. The figure at right shows the behavior of a single elastic element as the applied stress varies. The element, originally open with length L_o, closes to length L_c as the stress increases to σ_c, and it remains closed as the stress continues to increase. When the stress is decreased, the element opens at σ_o, changing back to length L_o and remaining there as stress decreases further. A large number of such elements with differing L_o, σ_o, L_c and σ_c models the heterogeneous elastic elements of the rock's bond system.

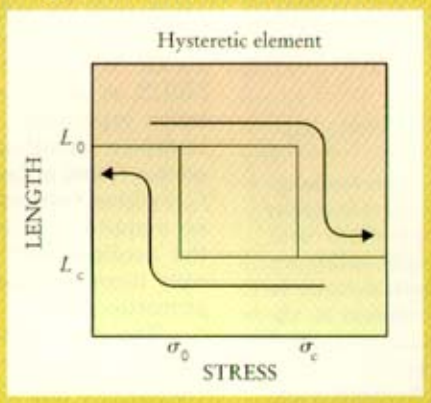

The stresses σ_o and σ_c for each element can be used as the element's coordinates in "P–M space," as shown at right. As the stress on the rock is varied, we can use P–M space to keep track of which elements are open and which are closed.

For instance, suppose the rock is taken through stress history $\sigma = 0, \sigma_A, \sigma_B, \sigma_{A'} (= \sigma_A), \sigma_C, \sigma_D, \sigma_{C'} (= \sigma_C), 0$. The bottom series of figures show the states of the elastic elements in P–M space for each stress (closed elements are black). The resulting stress–strain curve is shown at far right.

Initially, at $\sigma = 0$, the rock is elastic equilibrium. All of the elastic elements are in the open state. As the stress advances toward σ_B, elastic elements progressively close from left to right in P–M space, and the strain follows the lower curve. As the stress decreases from σ_B, the elements open from top to bottom, and the strain follows the upper curve.

The stress–strain cusp at B results from the difference between closing elastic elements ($A \rightarrow B$) and opening elastic elements ($B \rightarrow A'$). Compare the P–M space for A and A'. The stress is the same at both points, but the rock is in a different elastic state, with a different strain, in the two instances. Measurement of the elastic modulus (the slope of the stress–strain curve) in states A and A' would produce two distinct outcomes that tell about the different stress histories leading to the same stress state.

The phenomenon of discrete memory is illustrated in the loop $C \rightarrow D \rightarrow C'$ in the figure. This loop begins and ends at the same stress–strain point. The stress–strain trajectory of the outer loop is independent of the inner loop; the outer loop would be the same whether or not the inner loop is traversed.

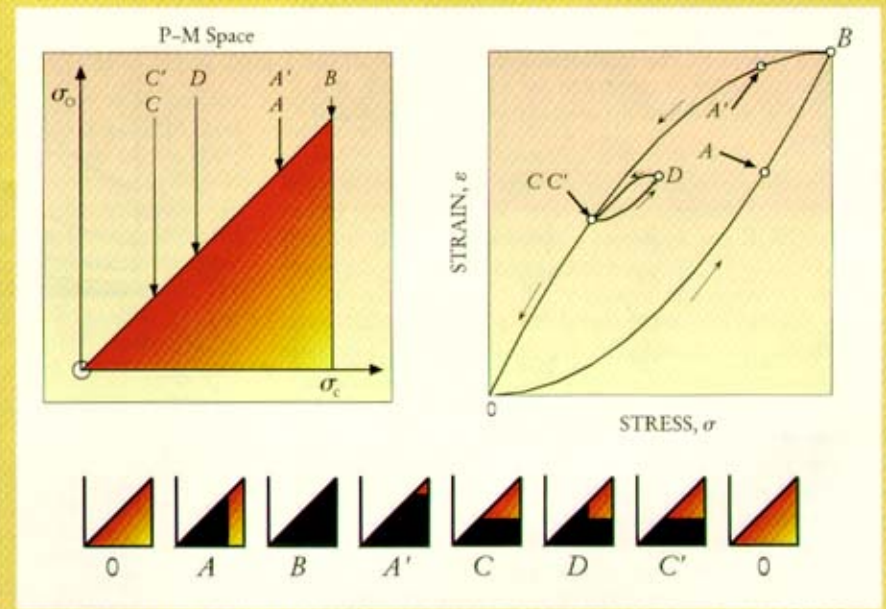

rial—above an elastically hard substrate. The soil layer amplifies an incident seismic wave because of both velocity contrasts and the layer's resonant response (much like a resonant bar).

Earthquake engineering attempts to mitigate damage to structures. One of its goals is to predict the Fourier components of the displacement at a location of interest, called the "site response." Buildings are then engineered so that their resonances are away from the peak frequencies of the site response. A rule of thumb such as "the fundamental period T_1 of an N-story building is $T_1 = 0.09N$ seconds" serves as an initial guide.[9] The prediction of site response can employ numerical modeling and laboratory studies of materials that buildings are situated on,[10] or, preferably, studies of seismic data taken at the site of interest.[11] The Fourier spectrum is expressed in terms of the spectral ratio described in box 3.

From a comparison between the calculated[12] and empirical[13] spectral ratios for one site (box 3), together with other field and laboratory observations, we conclude that many of the materials near Earth's surface belong to the proposed universality class. Earthquake engineering studies have great practical consequences, and characterizing the elasticity of the materials involved is fundamental.

Probing damaged materials

Finally, let us turn to nonlinear mesoscopic elasticity in nondestructive evaluation (NDE). Here we have a surprise: Evidence suggests that a damaged atomic elastic material responds like an NME material. When damaged, engine blocks, bearings, sophisticated composites and other materials display nonlinear mesoscopic elasticity that appears to be much like that in rock or concrete. Therefore, experimental and theoretical methods developed for NME materials can be employed in the study of damaged atomic elastic materials. Nonlinear studies of damages materials owe much to the work of a group at the Institute of Applied Physics in Nizhny Novgorod, Russia,[14] to the work of the NDE community dating back to at least 1979,[15] and to the work of many others, including our own collaborators at Los Alamos National Laboratory and elsewhere.[16]

Box 2. The Nonlinear Wave Equation

The wave equation expresses the driving force for the local displacement u as a power series in the strain $\varepsilon = \partial u/\partial x$:

$$\frac{\partial^2 u}{\partial t^2} = \frac{K_0}{\rho_0}\frac{\partial}{\partial x}\left[\frac{\partial u}{\partial x} + \beta\left(\frac{\partial u}{\partial x}\right)^2 + \delta\left(\frac{\partial u}{\partial x}\right)^3 + \cdots\right] + A[\varepsilon, \dot{\varepsilon}],$$

where ρ_0 is the density and $K_0 = \partial\sigma/\partial\varepsilon$ is the elastic modulus. Retaining only the first term on the right-hand side results in the linear wave equation. The nonlinear terms with amplitudes β, δ and so forth come from the traditional theory of nonlinear elastic waves. The hysteretic elastic elements in the bond system of the rock make a contribution to the motion of the displacement field that depends upon ε and $\dot{\varepsilon}$ and is typically nonanalytic; it is denoted by $A[\varepsilon, \dot{\varepsilon}]$.

The traditional nonlinear terms with amplitudes β, δ and so forth produce interactions among strain fields. For instance, the cubic anharmonicity term, with strength β, leads to an interaction between three strain fields in which two fields, of frequencies ω_1 and ω_2 and amplitudes ε_1 and ε_2, coalesce to form a third. The outgoing strain field has frequency components $\omega_3 = \omega_1 \pm \omega_2$ and amplitude ε_3 that is proportional to the product $\varepsilon_1\varepsilon_2$. Furthermore, when one strain wave with amplitude ε_1 and frequency ω_1 is propagating along a trajectory, the nonlinear coupling can create an outgoing strain wave at frequency 2ω with amplitude proportional to ε_1^2 that builds up over distance x to amplitude $\varepsilon_3(x) = \beta\varepsilon_1^2 x$.

	β	δ	A	Slow dynamics
Water	6	36	No	No
Copper	7	49	No	No
Rock	10^3	10^6	Yes	Yes
PZT5	4–5	10^4	No	No

Some appreciation for the distinction between materials with atomic elasticity (such as water and copper) and nonlinear mesoscopic elasticity (such as rock and PZT5, a ceramic composed of lead, zirconate and titanate that is used as an acoustic source) can be gleaned from the accompanying table, in which we give strengths β and δ of the cubic and quartic anharmonicities. We also indicate whether the hysteretic contribution A and slow dynamics—often a manifestation of nonlinear mesoscopic elasticity described in the text—are present.

Evidence of damage to an elastic material can be sought in a variety of ways, such as by studying the linear resonances, by employing wave propagation experiments or by using a general approach that we term nonlinear elastic wave spectroscopy (NEWS). (NEWS includes NRUS, as described above.) The result of a NEWS modulation experiment is shown in figure 5. When a sample is driven simultaneously at modest amplitude ε_1 at frequency f_1 and at large fixed amplitude ε_2 at high frequency f_2, nonlinear processes produce sidebands at $f_\pm = f_2 \pm f_1$ with an amplitude proportional to $\varepsilon_1\varepsilon_2$ and to the strength of the nonlinearity[16] When the amplitude ε_1 is systematically increased, the amplitude of the sidebands increases proportionally

The color contour plots in figure 5 are of the Fourier spectrum as a function of progressively increasing drive

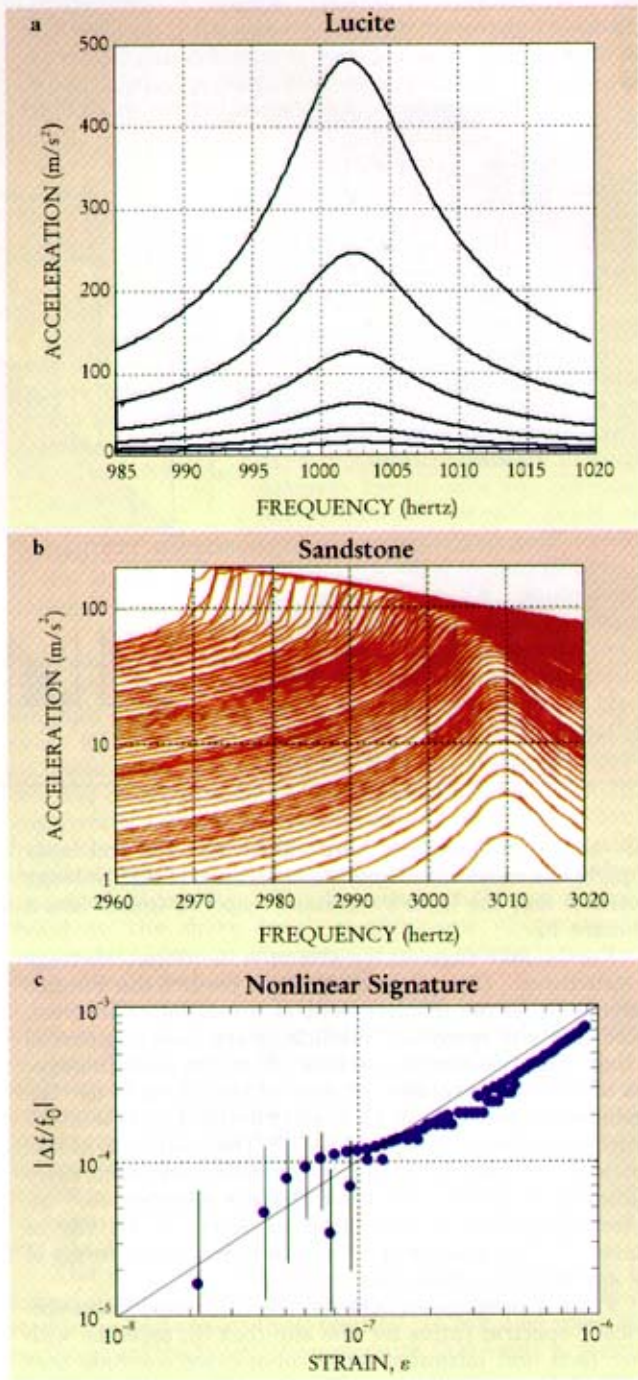

FIGURE 3. RESONANCE RESPONSE CURVES of atomic elastic and mesoscopic elastic materials. The detected acceleration amplitude of an acoustically driven sample is plotted as a function of frequency for a sequence of drive levels for Lucite (a) and for Berea sandstone (b). There is no evidence for change in the resonance response in Lucite as a function of drive level for acceleration amplitudes of up to 500 m/s², corresponding to strains of order 10^{-5}. The response of the sandstone is qualitatively different. As the drive is increased from a low level, the resonance curves become asymmetric, first slightly and then severely, while the resonance frequency shifts downward. c: The shift in the resonance frequency away from its value at low drive levels (f_0 = 3010 Hz) is a linear function of strain amplitude for the lowest strains measured, $3 \times 10^{-8} \le \varepsilon \le 10^{-6}$ (accelerations less than 30 m/s²), indicating that hysteresis in the equation of state is causing the nonlinearity. For higher strains, slow dynamics can be observed, in which the resonant frequency at low drive levels gradually shifts back to its original value after a large drive is removed.

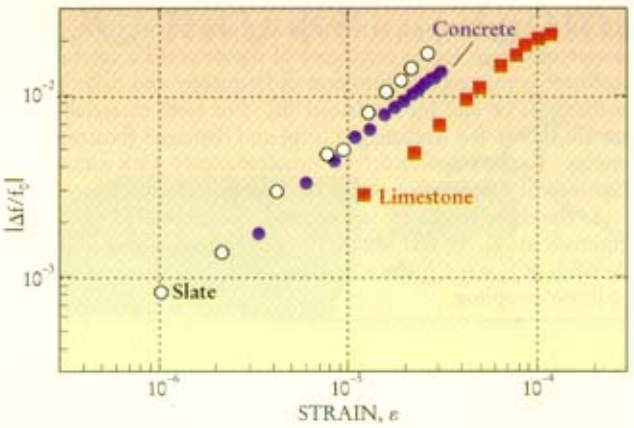

FIGURE 4. OTHER MATERIALS showing nonlinear mesoscopic elasticity include Lavoux limestone, concrete and synthetic slate (data courtesy of K. E.-A. Van Den Abeele). The resonant-bar response of each of these materials is qualitatively similar to that of sandstone and entirely unlike that of Lucite (see figure 3). The shift in resonant frequency for these materials is approximately linear in the strain amplitude and of magnitude consistent with the sandstone data in figure 3c.

level and frequency. For both Plexiglas and sandstone, the figure shows the results on two samples—one undamaged and one damaged. Undamaged Plexiglas, having atomic elasticity, shows the expected linear response: As the drive level ε_1 is increased, there is negligible spectral amplitude at frequencies $2f_1$ and f_-. In undamaged sandstone, which has nonlinear mesoscopic elasticity, as the drive level is increased, the spectral amplitudes at $2f_1$ and at $f_\pm$ increase. The contrast between the undamaged response spectra underscores the qualitative difference in the elastic behavior of the two classes of material.

This contrast disappears in the damaged samples. Both damaged samples in figure 5 show significant amplitudes at $f_\pm$, $2f_1$ and $3f_1$ (and even $5f_1$ in sandstone). There is nonlinearity in the Plexiglas that was absent when it was undamaged, and there is more nonlinearity in the damaged sandstone. The similarity of the damaged

Box 3. Spectral Ratios and Earthquake Engineering

For earthquake engineering, it is important to isolate the effects on ground motion amplitude that are due to local geology from those of the source spectrum and of the wave path. We can determine the local effects by considering seismic waves from an earthquake of strength S that is incident on two adjacent surface regions, one of uniformly elastically hard material and the other having a layer of nonlinear mesoscopic elastic (NME) material on top of elastically hard material. The time train of the surface ground motion is detected by geophones D_1, located on the surface of the NME layer, and D_2, located on the surface of the hard material. When the time trains are Fourier analyzed, the spectral ratio $R(\omega; S) = |D_1(\omega; S)|/|D_2(\omega; S)|$ gives the amplification due to the NME layer.

If the NME layer is elastically identical to the background, $R(\omega) = 1$ for all earthquakes. If the layer is elastically soft compared to the background but otherwise linear, $R(\omega)$ has a symmetric resonant peak with size proportional to the earthquake source strength S, similar to the Lucite bar (figure 3a). If the layer is an NME material with nonlinearity, hysteresis and discrete memory, $R(\omega)$ has a resonant peak whose shape and size depends on the magnitude of the earthquake, similar to the sandstone resonant bar (figure 3b).

In the absence of empirical data, we can use numerical modeling to predict the site response. The accompanying figure compares the calculated spectral ratio[12] to the empirical spectral ratio. The latter was constructed from seismograms recorded during the main shock and 18 aftershocks of the earthquake that struck the Northridge area in southern California on 17 January 1994.[13]

In the figure, the calculated site response is shown on the left as a function of frequency and input amplitude. The plot on the right shows the empirical site response of a strong-motion site (LF6) compared to a hard rock site (LWS). Redder colors correspond to higher amplification.

The model used in the simulation consisted of an NME layer, 100 m thick and much more than 100 m wide, over an elastically hard half-space. An equation of state incorporating nonlinearity, hysteresis and discrete memory was used for the NME layer. Although the surrounding rock is itself an NME material, it is much less nonlinear than the surface layer, and so it was modeled as a linear material. An empirical seismic signal, with frequency components between 0.2 and 20 Hz and varying amplitude corresponding to magnitudes of 2–7 on the Richter scale, was used both as the drive at the bottom of the NME layer and as the reference signal for the spectral ratio.

Both model and empirical site responses show a resonance in the range of 0.5–1 Hz. Although the real data are more complicated, the qualitative similarity of the two plots provides evidence that LF6 is a soft resonant layer site. The similarity of some details, such as the "toe" in the lower left corner in the left-hand plot—due to the mode mixing of strain waves in the layer—and the increased amplification at the lower left in the right-hand plot, suggests that physical mechanisms identified in numerical modeling are present at the strong-motion site.

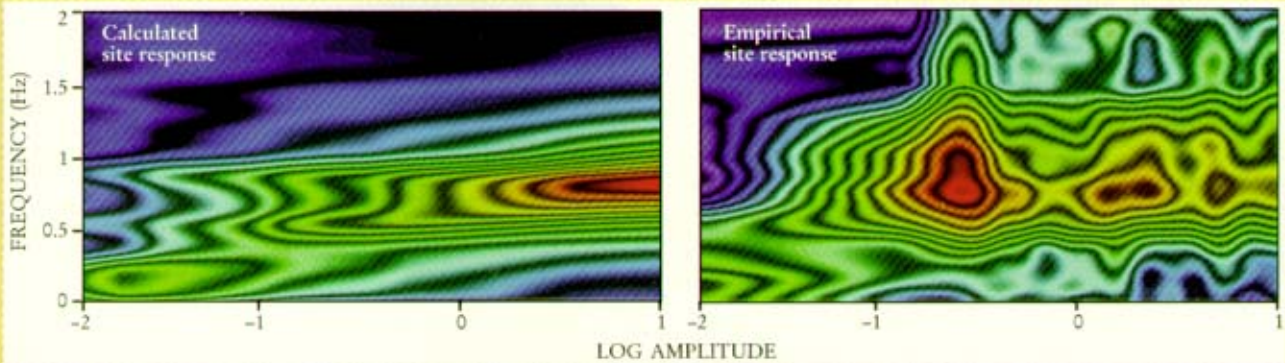

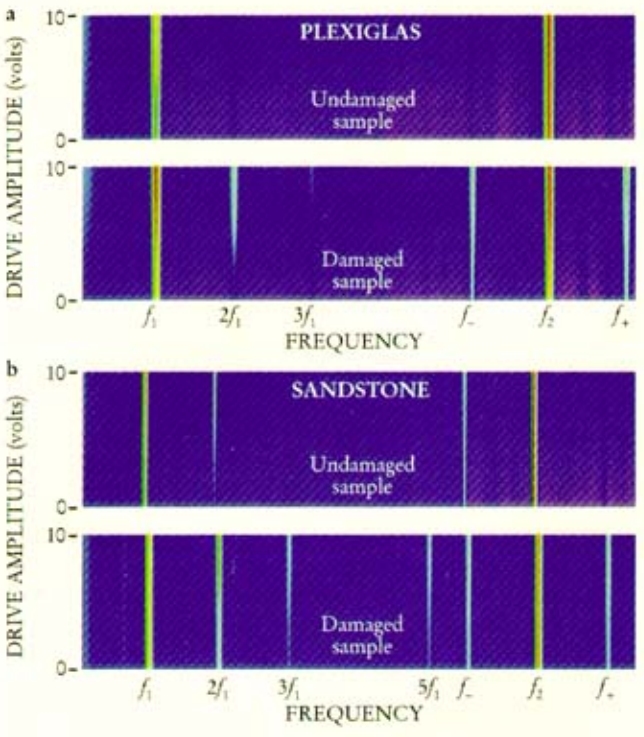

FIGURE 5. NONLINEAR ELASTIC WAVE SPECTROSCOPY. The Fourier spectrum (color contours) of the detected acceleration amplitude is plotted as a function of frequency and drive level, for Plexiglas (**a**) and for sandstone (**b**). For both materials, data are shown for undamaged (top) and damaged (bottom) samples. Each sample is driven simultaneously with a modest amplitude at frequency f_1 and a large amplitude at frequency f_2. As the drive level at f_1 is increased, the growth of the amplitude at $2f_1$, $3f_1$ and higher harmonics and at the sidebands at $f_- = f_2 - f_1$ show evidence of the presence of nonlinear coupling.

Plexiglas response to that of the sandstone suggests that the damage in the Plexiglas is associated with nonlinear coupling mechanisms similar to those operating in NME materials. Analysis of the scaling of the harmonic amplitudes with strain supports this suggestion.[16]

A work in progress

Experiments on rocks have revealed evidence for nonlinearity, hysteresis and discrete memory in their elastic behavior. Some elastic behavior observed in other materials, including soil, cement, concrete and damaged atomic elastic materials is similar, which has led us to suggest that there is a nonlinear mesoscopic elasticity universality class and to place all of these materials in it. There is no order parameter, symmetry or other parameter to show that this supposition is correct. Rather, there is the notion that the elastic properties of these materials have their source in qualitative features of a bond system that responds in a similar manner throughout the class. Such bond systems include the grain-to-grain contacts in rock, fluid-soaked contacts in a soil and the defect fabric of damaged atomic elastic material. It is these bond systems that endow NME materials with their defining properties.

Many challenges still remain in the study of these materials: understanding their behavior in the many practical contexts in which they are found, identifying those features that are essential to a proper mesoscopic description of the elastic behavior and understanding the underlying microscopic mechanisms that are responsible for it all.

R. A. Guyer is supported by the University of Massachusetts, Amherst and the Institute of Geophysics and Planetary Physics at LANL. P. A. Johnson is supported by the DOE Office of Basic Energy Research (Engineering and Geoscience) and by the Institute of Geophysics and Planetary Physics at Los Alamos National Laboratory. Thanks to our colleagues G. Boitnott, L. Byer, B. Hilbert, S. Levy, K. R. McCall, R. J. O'Connell, L. Ostrovsky, P. Rasolofosaon, T. J. Shankland, D. E. Smith, A. Sutin, J. A. TenCate, K. E.-A. Van Den Abeele, B. Zinszner and many others, as well as to High Mesa Petrographics for the thin section used in figure 1.

References

1. R. A. Guyer, K. R. McCall, G. N. Boitnott, Phys. Rev. Lett. **74**, 3491 (1995). K. R. McCall, R. A. Guyer, J. Geophys. Res. **99**, 23887 (1994).
2. L. D. Landau, E. M. Lifshitz, *Theory of Elasticity*, 3rd ed., Pergamon, Oxford, England (1986).
3. There exist many fine books and review articles on nonlinear acoustics, including R. T. Beyer, *Nonlinear Acoustics in Fluids, Benchmark Papers in Acoustics*, Van Nostrand Reinhold, New York (1984); M. F. Hamilton, D. T. Blackstock, eds., *Nonlinear Acoustics*, Academic, San Diego (1997); K. Naugolnykh, L. Ostrovsky, *Nonlinear Wave Processes in Acoustics*, Cambridge U. P., New York (1998); L. K. Zarembo, V. A. Krasil'nikov, *Sov. Phys. Usp.* **13**, 778 (1971).
4. G. D. Meegan Jr, P. A. Johnson, K. R. McCall, R. A. Guyer, J. Acoust. Soc. Am. **94**, 3387 (1993). J. A. TenCate, K. E.-A. Van Den Abeele, T. J. Shankland, P. A. Johnson, J. Acoust. Soc. Am. **100**, 1383 (1996). K. E.-A. Van Den Abeele, J. Acoust. Soc. Am. **99**, 3334 (1996).
5. T. Cadoret, D. Marion, B. Zinszner, J. Geophys. Res. **100**, 9789 (1995).
6. O. L. Anderson, D. G. Isaak, in *A Handbook of Physical Constants: Mineral Physics and Crystallography*, AGU Reference Shelf vol. 2, T. J. Ahrens, ed., American Geophysical Union, Washington, DC (1995), p. 64. A. Migliori, J. L. Sarrao, *Resonant Ultrasound Spectroscopy: Applications to Physics, Materials Measurements, and Non-Destructive Evaluation*, Wiley, New York (1997).
7. J. A. TenCate, T. J. Shankland, Geophys. Res. Lett. **23**, 3019 (1996).
8. I. A. Beresnev, K.-L. Wen, Bull. Seismol. Soc. Am. **86**, 1964 (1996). K. Ishihara, *Soil Behavior in Earthquake Geotechnics*, Clarendon, Oxford, England (1996).
9. T. Paulay, M. J. N. Priestley, *Seismic Design of Reinforced Concrete and Masonry Buildings*, Wiley, New York, (1992).
10. M. Vucetic, R. Dobry, J. Geotechnical Eng. **117**, 89 (1991). G. Yu, J. G. Anderson, R. Siddharthan, Bull. Seismol. Soc. Am **83**, 218 (1993).
11. A.-W. Elgamal, M. Zeghal, E. Parra, R. Gunturi, H. T. Tang, J. C. Stepp, Soil Dynamics and Earthquake Engineering **15**, 499 (1996).
12. K. E.-A. Van Den Abeele, P. A. Johnson, F. Bonilla, E. H. Field, I. Beresnev, preprint available.
13. E. H. Field, Y. Zeng, P. A. Johnson, I. A. Beresnev, J. Geophys. Res. **103**, 26869 (1998).
14. A. S. Korotkov, M. M. Slavinskii, A. M. Sutin, Acoust. Phys. **40**, 71 (1994). A. S. Korotkov, A. M. Sutin, Acoust. Lett. **18**, 59 (1994).
15. W. L. Morris, O. Buck, R. V. Inman, J. Appl. Phys. **50**, 6737 (1979). The papers presented at the annual Quantitative Nondestructive Evaluation meeting represent a wealth of information. See, for example, D. O. Thompson, D. E. Chimenti, eds., *Review of Progress in Quantitative Nondestructive Evaluation Vol. 11*, Plenum, New York (1992).
16. P. A. Johnson, A. Sutin, K. E.-A. Van Den Abeele, preprint available.
17. F. Preisach, Z. Phys. **94**, 277 (1935). I. D. Mayergoyz, J. Appl. Phys. **57**, 3803 (1985). ■